

Pseudorapidity dependence of short-range correlations from a multi-phase transport model

Wang Meijuan^{1*}, CHEN Gang¹ Ma Guoliang² Wu Yuanfang³

¹*Physics Department, China University of Geoscience, Wuhan 430074, China*

²*Shanghai Institute of Applied Physics, Chinese Academy of Sciences, Shanghai 201800, China*

³*Key Laboratory of Quark and Lepton Physics (MOE) and Institute of Particle Physics, Central China Normal University, Wuhan 430079, China*

Using a multi-phase transport model (AMPT) that includes both initial partonic and hadronic interactions, we study neighboring bin multiplicity correlations as a function of pseudorapidity in Au+Au collisions at $\sqrt{s_{NN}} = 7.7 - 62.4$ GeV. It is observed that for $\sqrt{s_{NN}} < 19.6$ GeV Au+Au collisions, the short-range correlations of final particles have a trough at central pseudorapidity, while for $\sqrt{s_{NN}} > 19.6$ GeV Au+Au collisions, the short-range correlations of final particles have a peak at central pseudorapidity. Our findings indicate that the pseudorapidity dependence of short-range correlations should contain some new physical information, and are not a simple result of the pseudorapidity distribution of final particles. The AMPT results with and without hadronic scattering are compared. It is found that hadron scattering can only increase the short-range correlations to some level, but is not responsible for the different correlation shapes for different energies. Further study shows that the different pseudorapidity dependence of short-range correlations are mainly due to partonic evolution and the following hadronization scheme.

PACS numbers: 25.75.-q, 24.85.+p, 24.10.Lx

I. INTRODUCTION

The main goal of high energy heavy ion collision experiments is to investigate the nuclear matter properties under extreme conditions and detect quark-gluon plasma (QGP). It has been confirmed that QGP is produced in relativistic heavy ion collisions [1, 2]. Many observables have been used to study and compare the properties of nuclear matter with and without QGP, such as the strong anisotropic collective flow [3], nuclear modification factor R_{AA} [4] and so on.

If a shortening in the correlation length in pseudorapidity space is observed, it may be taken as a signal of transition to quark-gluon plasma [5]. Therefore, particle correlations are also of particular importance for the study of QGP properties. It has been reported that inclusive two-particle correlations have two components: short-range correlations (SRC) and long-range correlations (LRC), corresponding to small and large pseudorapidity differences, respectively.

Forward-backward correlations, as a special case of long-range correlations, have been extensively studied in elementary particle collisions [6] [7] and by the STAR experiment in heavy ion collisions at RHIC [8]. Because they probe the longitudinal characteristics of the system produced in heavy ion collisions, they provide an insight into space-time dynamics and the earliest stages of particle production.

In comparison to the well-investigated long-range correlations that determine the bulk properties of the collision system, short-range correlations have a more sub-

tle influence on the in-medium properties of the particles [9] [10]. It is believed that in pp collisions SRC arise due to the tendency of the secondary particles to be grouped in clusters, which finally decay to the real physical hadrons [11] [12]. To our knowledge, few studies have been done about SRC in Au+Au collisions.

In this study, we will focus on the pseudorapidity dependence of short-range correlations in Au+Au collisions. We will utilize a multi-phase transport (AMPT) model [13] to simulate Au+Au collisions at RHIC, and try to record a complete system evolution. The pseudorapidity dependence of short-range correlations for the following cases are measured: (1) the effects of initial state; (2) the early partonic phase; (3) the intermediate hadronic phase, the time when the collision system undergoes the hadronization, while hadronic scattering scheme is closed; (4) the hadronic phase, when hadronization has happened and the hadronic scattering scheme is open. These can present a clear image of short-range correlations for different states of the collision system, especially for the partonic phase and hadronic phase.

This paper is organized as follows. A short introduction of the AMPT model is given in Section II. In Section III, we present the AMPT results for the pseudorapidity dependence of neighboring-bin correlation patterns in Au+Au collisions at $\sqrt{s_{NN}} = 7 - 62.4$ GeV. We discuss the effects of both the partonic and hadronic evolutions, and take $\sqrt{s_{NN}} = 7.7$ GeV and 62.4 GeV as two examples to focus on the influence of parton phase evolution on the short range pseudorapidity correlation patterns. Finally, some conclusions are given in Section IV.

*wangmj@cug.edu.cn

II. A BRIEF INTRODUCTION TO THE AMPT MODEL

The Monte Carlo event generator AMPT (A Multi-Phase Transport) has been used in this study. The AMPT model is made up of four main components: initial conditions, partonic interactions, hadronization and hadronic interactions. The initial conditions, which include the spatial and momentum distributions of mini-jet partons from hard processes and strings from soft processes, are obtained from the Heavy Ion Jet Interaction Generator (HIJING) model [14]. The evolution of partonic phase is modeled by Zhang's Parton Cascade (ZPC) [15], which includes only parton-parton elastic scatterings with cross sections obtained from the pQCD calculation with screening masses. The AMPT model has two versions, the default AMPT model and the AMPT model with string melting mechanism. In the default AMPT model, only mini-jet partons from the initial conditions take part in the interactions modeled by ZPC. When stopping interactions, they are combined with their parent strings to form new strings. The resulting strings are then converted to hadrons according to a Lund string fragmentation model [16, 17]. In the AMPT model with string melting, the parent strings first fragment into partons and then enter the ZPC model together with the mini-jet partons. After freezing out, a simple quark coalescence model is used to combine the two nearest partons into a meson and three nearest partons into a baryon [18]. For both versions of the AMPT model, the interactions among resulting hadrons are described by a relativistic transport (ART) model [19].

Compared with the default AMPT model, the partonic phase can be better modeled by the AMPT model with string melting mechanism. Because the QGP is expected to be formed in heavy-ion collisions at the Relativistic Heavy-Ion Collider (RHIC), the AMPT with string melting mechanism is considered a more efficient tool to study the properties of the new matter, e.g. studying the elliptic flow and triangular flow [20]. Based on this, we will utilize the AMPT model with string melting mechanism to generate Au+Au collisions at $\sqrt{s_{NN}} = 7.7 - 62.4$ GeV. The parton cross section is taken to be 10 mb in our simulations.

III. NEIGHBORING RAPIDITY BIN MULTIPLICITY CORRELATION

One focus of the analysis of the final state is on the longitudinal momentum distributions, and correlations. In this section, we show the variation in particle density with η . Then, we mainly study the pseudorapidity dependence of neighboring bin multiplicity at different colliding energies.

Figure 1 shows the pseudorapidity distributions of final particles within $-5 \leq \eta \leq 5$ in Au+Au collisions at $\sqrt{s_{NN}} = 7 - 62.4$ GeV. As expected the particle density

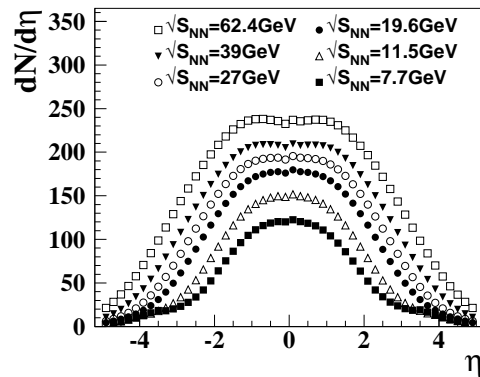


FIG. 1: The pseudorapidity distribution of final particles at $\sqrt{s_{NN}} = 7.7 - 62.4$ GeV Au+Au collisions using the AMPT model with string melting mechanism.

increases with decrease in η for all energies. In addition, as a function of collision energy, we can see the pseudorapidity distribution grows systematically both in height and width.

The general two-bin multiplicity correlation is defined as

$$C_{1,2} = \frac{\langle n_1 n_2 \rangle}{\langle n_1 \rangle \langle n_2 \rangle} - 1, \quad (1)$$

where n_1 and n_2 are the numbers of particles measured in bin 1 and bin 2. If particles are produced independently over the whole region, then $\langle n_1 n_2 \rangle = \langle n_1 \rangle \langle n_2 \rangle$ and correlations vanish.

It has previously been demonstrated that two specific 2-dimensional correlation pattern, i.e. fixed-to-arbitrary and neighboring bin correlation patterns, are efficient for identifying various random multiplicative cascade processes [21].

In this work, we apply the neighboring bin pseudorapidity correlation pattern to the relativistic heavy-ion collisions, proposing the following form

$$C(\eta) = \frac{\langle n_\eta n_{\eta+\delta\eta} \rangle}{\langle n_\eta \rangle \langle n_{\eta+\delta\eta} \rangle} - 1, \quad (2)$$

where $\delta\eta$ corresponds to the width of the bins, η and $\eta + \delta\eta$ are the center of the two bins, and n_η and $n_{\eta+\delta\eta}$ correspond to the multiplicities of the two bins. In the following, the mid-rapidity $[-2, +2]$ is chosen and we divide the region equally into 20 bins, which corresponds to the bin width $\delta\eta = 0.2$. It is clear that the neighboring bin multiplicity correlation pattern can demonstrate how the short range correlations vary with the pseudorapidity.

Figure 2 presents the AMPT results for the dependence of neighboring bin correlation patterns for Au+Au collisions at $\sqrt{s_{NN}} = 7.7, 11.5, 19.6, 27, 39$ and 62.4 GeV. We calculate two cases of correlations, i.e. (a) w-ART, which represents the results from a complete time evolution process of the AMPT model, as shown by solid

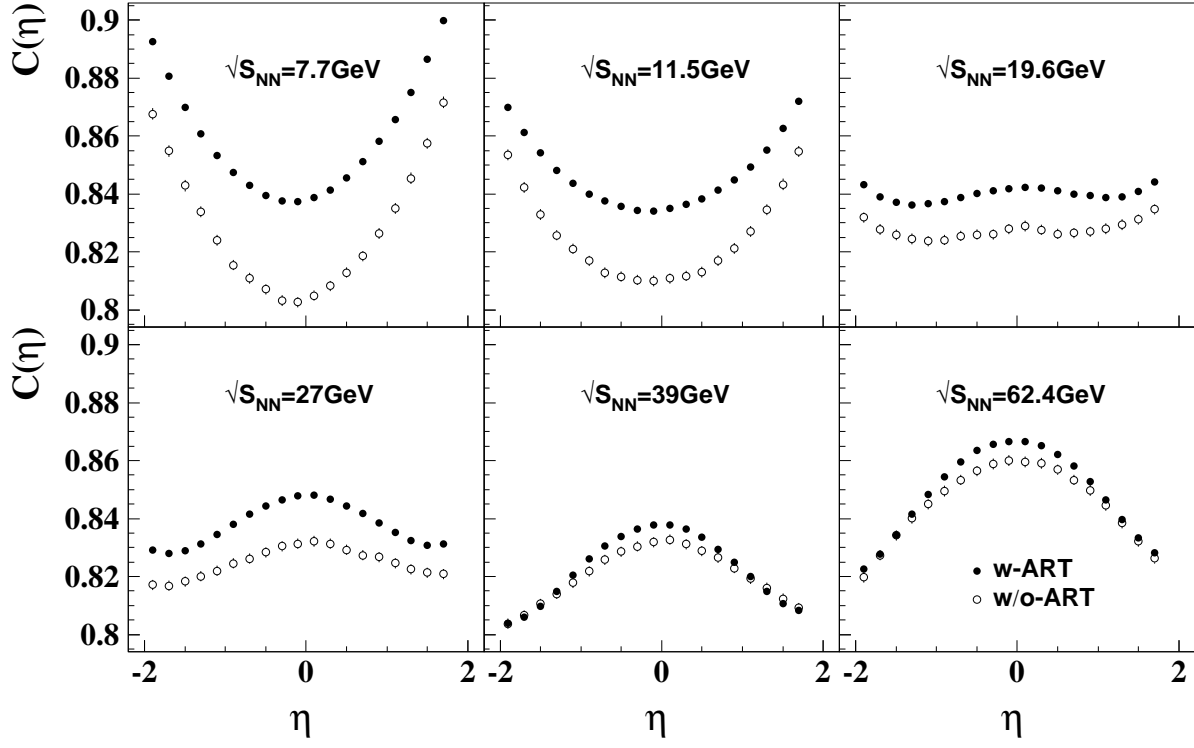


FIG. 2: The pseudorapidity dependence of neighboring bin correlation pattern at $\sqrt{s_{NN}} = 7.7 - 62.4$ GeV Au+Au collisions using the AMPT model with string melting mechanism, where the solid points and open points correspond to the result with and without hadronic scattering respectively.

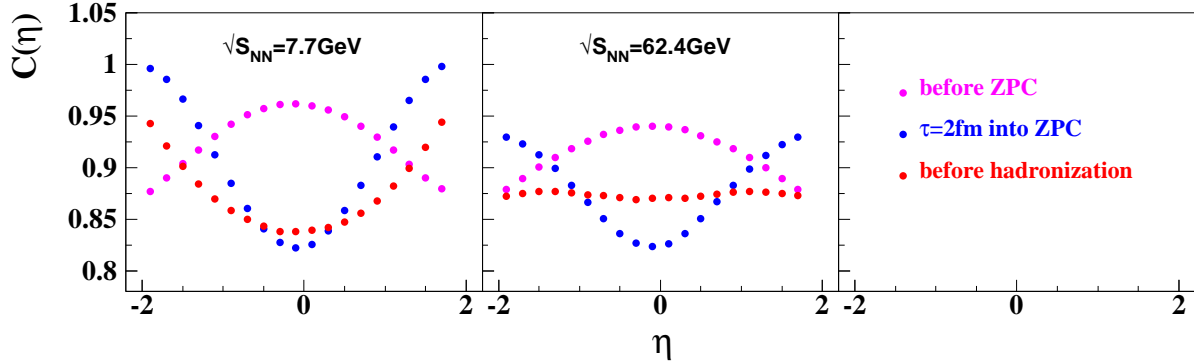


FIG. 3: The pseudorapidity dependence of neighboring bin correlation pattern for partons at $\sqrt{s_{NN}} = 7.7$ GeV and 62.4 GeV Au+Au collisions using the AMPT model with string melting mechanism, where different colors correspond to the correlation results from different evolution times.

circles; (b) w/o-ART represents the results from the time just after quark coalescence, but before hadronic scatterings, shown as open circles. Comparing these two cases, can help us understand the hadronic effect on the observable. From the figure, we can see the neighboring bin correlation patterns have a different dependence on the pseudorapidity at different colliding energies. We can see that both w-ART and w/o-ART show that the correlation strength first decreases and then increases with the pseudorapidity, and has a minimum value at the central pseudorapidity for Au+Au collisions at $\sqrt{s_{NN}} =$

7.7 and 11.5 GeV, while it first increases and then decreases, with a maximum at the central pseudorapidity, for Au+Au collisions at $\sqrt{s_{NN}} = 27, 39$ and 62.4 GeV. For Au+Au collisions at $\sqrt{s_{NN}} = 19.6$ GeV, the correlation patterns have little dependence on the pseudorapidity. It is well known that the pseudorapidity distribution has a plateau at mid-rapidity for all energies, as shown in Figure 1, thus we believe that the pseudorapidity dependence of short range correlations should contain some new physical information, but is not a simple result of the pseudorapidity distribution of particles. From the

figure, we can see the results from w/o-ART are lower than that those w-ART for all collision energies, which means hadronic scattering can increase the correlation strength to some level. In addition, the values of w/o-ART are closer to those of w-ART at higher energies. This indicates that hadronic interactions have little effect on the correlation patterns at very high energies.

As we know, the AMPT model is a hybrid model, in which hadronic and partonic interactions are both included [13]. It is widely believed that hadronic interactions dominate the correlation behaviors at low energies and partonic interactions dominate the correlation behaviors at high energies [22]. In Figure 2, we learn that there exist different correlation behaviors for different energies, and that hadronic interactions only have an effect on the correlation strength, cannot explain the different pseudorapidity dependence of short-range correlations with collision energy. Further study is needed.

Next, Au+Au collisions at $\sqrt{s_{NN}} = 7.7\text{GeV}$ and 62.4GeV are chosen to study the effect of the partonic phase on the correlation behavior, since they correspond to the two cases for low and high energy respectively. In Figure 3, we present the pseudorapidity distribution of short-range correlations between partons for the two energies at different partonic evolution times. Three important evolution times are considered. The before ZPC represents the short range correlation pattern from the initial state of partonic matter; $\tau = 2fm/c$ into ZPC describes the short-range correlation pattern at the time point when the partonic phase evolution has been going on for $2 fm/c$. The before hadronization presents the short-range correlation pattern from the moment when all of partons freeze out before hadronization.

From Figure 3, we can see that the short-range correlations first increase and then decrease with pseudorapidity both for 7.7GeV and 62.4GeV for the initial state of the colliding system (i.e. before ZPC). For $\tau = 2fm/c$ into ZPC, it is interesting to note that the correlation patterns show the reversal effect, as they first decrease and then increase with pseudorapidity for both energies. When the partons stop interactions (before hadronization), however, there is a significant difference for Au+Au collisions at 7.7 GeV and 62.4 GeV . For 7.7GeV Au+Au collisions, the short-range correlations continue to keep a curved upward trend with pseudorapidity, while for 62.4GeV Au+Au collisions, the short-range correlations are not sensitive to the pseudorapidity. This can be explained by the fact that for $\sqrt{s_{NN}} = 62.4\text{GeV}$ Au+Au collisions there exist enough interactions between partons to drive the colliding system into isotropy.

After partons in the string melting scenario stop interacting, their hadronization is modeled via a simple quark coalescence[18]. In the quark coalescence model, we can combine the two nearest partons into a meson and three nearest quarks into a baryon. Related research[23] has shown that the total yield of the meson (baryon) is proportional to the square (cube) of quark density

just before hadronization. We argue that correlation of final particles is also related to the constituent quark density in the hadronization process. By combining the nearest quarks into hadrons, the hadronization scheme of quark coalescence can obviously increase short-range correlations, and the influence of the hadronization process on short-range correlations strongly depends on the quark density just before hadronization. For $\sqrt{s_{NN}} = 62.4\text{GeV}$ Au+Au collisions, the flat correlation pattern as shown in Figure 3 become a shape curved downward after hadronization, due to stronger short-range correlations from the larger quark density at central pseudorapidity just before hadronization. However, because only a limited number of partons pass through hadronization for 7.7 GeV Au+Au collisions, the weak influence doesn't change the correlation shape and it keep a shape curved upward. By combining the effects of partonic evolution and the subsequent quark coalescence scheme, the different pseudorapidity dependence of neighboring bin correlation patterns at different energies, as shown in Figure 2, is understandable.

IV. CONCLUSIONS

In summary, the pseudorapidity dependence of neighboring bin multiplicity correlation patterns are studied in a multi-phase transport model with both partonic and hadronic interactions. It is shown that the short-range correlations vary significantly with pseudorapidity for different energy regions. In particular, for $\sqrt{s_{NN}} < 19.6\text{GeV}$ Au+Au collisions, the short-range correlations have a trough at central pseudorapidity, while for $\sqrt{s_{NN}} > 19.6\text{GeV}$ Au+Au collisions, the short-range correlations of final particles have a peak at central pseudorapidity. The AMPT results with and without hadronic scattering are compared. It is found that hadron scattering can only increase the short-range correlations to some level, but is not responsible for the different correlation shapes for different energies. Further study shows the differences in pseudorapidity dependence of short-range correlations are mainly due to partonic evolution and the following quark coalescence mechanism. We argue that the neighboring bin multiplicity pseudorapidity correlation patterns are sensitive to the dynamics mechanism of the collision system evolution, and especially have a different response to the partonic phase and hadronic phase.

V. ACKNOWLEDGMENTS

The author Wang Meijuan thanks Xu Mingmei and Zhou You for useful discussion. This work were supported by GBL31512, Major State Basic Research Development Program of China under Grant No. 2014CB845402, the NSFC of China under Grants No.11475149, No. 11175232, No. 11375251, No.

11421505 and No. 11221504.

-
- [1] J. Adams et. al. (STAR Collab.), Nucl. Phys. A, 2005, **757**, 102.
 - [2] K. Adcox et. al. (PHENIX Collab.), Nucl. Phys. A, 2005, **757**, 184.
 - [3] J. Adams et al. (STAR Collab.), Phys. Rev. Lett., 2004, **92**, 052302; S. S. Adler et al. (PHENIX Collab.), Phys. Rev. Lett., 2003, **91**, 182301.
 - [4] S. S. Adler et al. (PHENIX Collaboration), Phys. Rev. Lett., 2003, **91**, 172301.
 - [5] V. P. Konchakovski et al., Phys. Rev. C, 2009, **79**, 034910.
 - [6] R. Akers et al., Phys. Lett. B, 1994, **320**, 417.
 - [7] W. Kittel and E. A. De. Wolf, Soft Multihadron Dynamics, World Scientific, 2005, 652.
 - [8] B. Abelev et al. (STAR Collaboration), Phys. Rev. Lett., 2009, **103**, 172301.
 - [9] Frank Froemel, Horst Lenske, Ulrich Mosel, Nucl. Phys. A, 2003, **723**, 544-556.
 - [10] Frank Froemel, Stefan Leupold, Phys. Rev. C, 2007, **76**, 035207.
 - [11] P. L. Jain, K. Sengupta, G. Singh, Phys. Rev. D, 1986, **34**, 2886-2889.
 - [12] KLM Collab. (M. L. Cherry), Acta. Phys. Pol. B, 1998, **29**, 2129.
 - [13] Zi-Wei Lin, C. M. Ko and Subrata Pal, Phys. Rev. Lett., 2002, **89**, 152301. Zi-Wei Lin, Che Ming Ko, Bao-An Li and Bin Zhang and Subrata Pal, Phys. Rev. C, 2005, **72**, 064901.
 - [14] X. N. Wang, Phys. Rev. D, 1991, **43**, 104; X. N. Wang and M. Gyulassy, Phys. Rev. D, 1991, **44**, 3501; X. N. Wang and M. Gyulassy, Phys. Rev. D, 1992, **45**, 844; M. Gyulassy and X. N. Wang, Comput. Phys. Commun., 1994, **83** 307.
 - [15] B. Zhang, Comput. Phys. Commun., 1998, **109**, 193.
 - [16] B. Andersson, G. Gustafson and B. Soderberg, Z. Phys. C, 1983, **20**, 317.
 - [17] T. Sjostrand, Comput. Phys. Commun., 1994, **82**, 74.
 - [18] L. W. Chen and C. M. Ko, Phys. Lett. B, 2006, **634**, 205.
 - [19] B. A. Li and C. M. Ko, Phys. Rev. C, 1995, **52**, 2037; B. A. Li, A. T. Sustich, B. Zhang and C. M. Ko, Int. J. Phys. E, 2001, **10**, 267.
 - [20] L. Ma, G. L. Ma, Y. G. Ma, Phys. Rev. C, 2014, **89**, 044907. Adam Bzdak, Guo-Liang Ma, Phys. Rev. Lett., 2014, **113**, 252301.
 - [21] Yuanfang Wu, Lianshou Liu, Yingdan Wang, Yuting Bai and Hongbo Liao, Phys. Rev. E, 2005, **71**, 017103.
 - [22] N. Xu (STAR Collaboration), Nucl. Phys. A, 2014, **931**, 1-12.
 - [23] C. B. Yang, J. Phys. G, (2006), **32**, L11.